PHYSICAL REVIEW D **92,** 073016 (2015)

Probing lepton nonuniversality in tau neutrino scattering

Hongkai Liu,[1,*] Ahmed Rashed,[1,2,3,†] and Alakabha Datta[1,‡]

[1]*Department of Physics and Astronomy, University of Mississippi, Lewis Hall, University, Mississippi 38677, USA*

[2]*Department of Physics, Faculty of Science, Ain Shams University, Cairo 11566, Egypt*

[3]*Center for Fundamental Physics, Zewail City of Science and Technology, 6 October City, Giza, Egypt*

(Received 28 May 2015; published 23 October 2015)

Recently hints of lepton flavor nonuniversality emerged in the *BABAR* and LHCb experiments. In this paper we propose tests of lepton universality in ν_τ scattering. To parametrize the new physics we adopt an effective Lagrangian approach and consider the neutrino deep inelastic scattering processes $\nu_\tau + N \to \tau + X$ and $\nu_\mu + N \to \mu + X$ where we assume the largest new physics effects are in the τ sector. We also consider an explicit leptoquark model in our calculations. In order to make comparison with the standard model and also in order to cancel out the uncertainties of the parton distribution functions, we consider the ratio of total and differential cross sections of tau-neutrino to muon-neutrino scattering. We find new physics effects that can possibly be observed at the proposed Search for Hidden Particles (SHiP) experiment at CERN.

DOI: 10.1103/PhysRevD.92.073016 PACS numbers: 13.15.+g, 12.60.-i

I. INTRODUCTION

The flavor sector of standard model (SM) has many puzzles. A key property of the SM gauge interactions is that they are lepton flavor universal. Evidence for violation of this property would be a clear sign of new physics (NP) beyond the SM. In the search for NP, the second and third generation quarks and leptons could be special because they are comparatively heavier and are expected to be relatively more sensitive to NP. As an example, in certain versions of the two Higgs doublet models (2HDM) the couplings of the new Higgs bosons are proportional to the masses and so NP effects are more pronounced for the heavier generations. Moreover, the constraints on new physics, especially involving the third generation leptons and quarks, are somewhat weaker allowing for larger new physics effects.

Interestingly, there have been some reports of nonuniversality in the lepton sector from experiments. Recently, the *BABAR* Collaboration with their full data sample has reported the following measurements [1,2]:

$$R(D) \equiv \frac{\mathcal{B}(\bar{B} \to D^+ \tau^- \bar{\nu}_\tau)}{\mathcal{B}(\bar{B} \to D^+ \ell^- \bar{\nu}_\ell)} = 0.440 \pm 0.058 \pm 0.042,$$
$$R(D^*) \equiv \frac{\mathcal{B}(\bar{B} \to D^{*+} \tau^- \bar{\nu}_\tau)}{\mathcal{B}(\bar{B} \to D^{*+} \ell^- \bar{\nu}_\ell)} = 0.332 \pm 0.024 \pm 0.018, \quad (1)$$

where $\ell = e, \mu$. The SM predictions are $R(D) = 0.297 \pm 0.017$ and $R(D^*) = 0.252 \pm 0.003$ [1,3], which deviate from the *BABAR* measurements by 2σ and 2.7σ, respectively. [The *BABAR* Collaboration itself reported a 3.4σ deviation from SM when the two measurements of Eq. (1) are taken together.] This measurement of lepton flavor nonuniversality, referred to as the $R(D^{(*)})$ puzzles, may be providing a hint of the new physics (NP) believed to exist beyond the SM. There have been numerous analyses examining NP explanations of the $R(D^{(*)})$ measurements [4,5].

In another measurement the LHCb Collaboration recently measured the ratio of decay rates for $B^+ \to K^+ \ell^+ \ell^-$ ($\ell = e, \mu$) in the dilepton invariant mass-squared range $1\ \text{GeV}^2 \le q^2 \le 6\ \text{GeV}^2$ [6]. They found

$$R_K \equiv \frac{\mathcal{B}(B^+ \to K^+ \mu^+ \mu^-)}{\mathcal{B}(B^+ \to K^+ e^+ e^-)} = 0.745^{+0.090}_{-0.074}(\text{stat}) \pm 0.036(\text{syst}), \quad (2)$$

is a 2.6σ difference from the SM prediction of $R_K = 1 \pm O(10^{-4})$ [7]. In addition, we note that the three-body decay $B^0 \to K^* \mu^+ \mu^-$ by itself offers a large number of observables in the kinematic and angular distributions of the final-state particles, and it has been argued that some of these distributions are less affected by hadronic uncertainties [8]. Interestingly, the measurement of one of these observables shows a deviation from the SM prediction [9]. However, the situation is not clear whether this anomaly is truly a first sign of new physics [10].

The tau neutrino, ν_τ, was discovered by the DONuT experiment [11] which measured the charged-current (CC) interaction cross section of the tau neutrino. The DONuT central-value results for the ν_τ scattering cross section show deviation from the standard model predictions by about 40% but with large experimental errors; thus, the measurements are consistent with the standard model. The third generation lepton has been explored relatively less than the

*hliu2@go.olemiss.edu
†amrashed@go.olemiss.edu
‡datta@phy.olemiss.edu

other two generations and in particular there has not been much investigation of ν_τ properties. One of the predictions of the standard model (SM) is that gauge bosons couple to the three generations of leptons universally. A careful test of this prediction is very important and observation of nonuniversality in the interactions of the lepton families would be an important discovery.

In previous publications we considered new physics in ν_τ scattering for quasiexclusive, resonant and deep inelastic scattering (DIS) [12]. In those papers we were more focused on the error in the extraction of neutrino mixing angles in presence of new physics. In this paper we focus on observables that may be measured at a ν_τ scattering experiment. There is a proposed Search for Hidden Particles (SHiP) experiment at CERN [13] which is expected to have a large sample of tau neutrinos which could be used to probe new physics in ν_τ scattering. In our previous work we did not include new physics tensor interactions which we consider in this work. In this work we will be interested at neutrino energies where the DIS component of the scattering process is dominant.

We start with an effective Hamiltonian description of new physics operators. We fix the constraints on the couplings from charged current τ decays. We will consider the decays $\tau \to \pi\nu_\tau$ and $\tau \to \pi\pi\nu_\tau$ which are well measured. We will finally consider an explicit leptoquark model where both scalar and tensor interactions, with relations between the couplings of the two interactions, are present.

The paper is organized in the following manner. In Sec. II we introduce the effective Lagrangian to parametrize the NP operators, describe the formalism of the decay process and introduce the relevant observables. In Sec. III we present our results and in Sec. IV we present our conclusions. We collect some of our equations in Appendix A.

II. FORMALISM

In the presence of NP, the effective Hamiltonian for the scattering process $\nu_\tau + N \to \tau + X$ can be written in the form [14],

$$\begin{aligned}\mathcal{H}_{\text{eff}} = \frac{4G_F V_{ud}}{\sqrt{2}}[(1+V_L)[\bar{u}\gamma_\mu P_L d][\bar{l}\gamma^\mu P_L \nu_l] \\ + V_R[\bar{u}\gamma^\mu P_R d][\bar{l}\gamma_\mu P_L \nu_l] + S_L[\bar{u}P_L d][\bar{l}P_L\nu_l] \\ + S_R[\bar{u}P_R d][\bar{l}P_L\nu_l] + T_L[\bar{u}\sigma^{\mu\nu}P_L d][\bar{l}\sigma_{\mu\nu}P_L\nu_l]],\end{aligned} \tag{3}$$

where $G_F = 1.1663787(6) \times 10^{-5}$ GeV^{-2} is the Fermi coupling constant, $V_{qq'}$ is the Cabibbo-Kobayashi-Maskawa (CKM) matrix element, $P_{L,R} = (1 \mp \gamma_5)/2$ are the projectors of negative/positive chiralities. We use $\sigma_{\mu\nu} = i[\gamma_\mu, \gamma_\nu]/2$ and assume the neutrino to be always left chiral. To introduce nonuniversality the NP couplings are in general different for different lepton flavors. We assume the NP effect is mainly through the τ lepton. The effective Hamiltonian involves the quarks of the first generations only. It is possible that the quarks of the other generations will also be affected by new physics. We will not assume any connection between new physics for the different generations of quarks. The SM effective Hamiltonian corresponds to $g_L = g_R = g_S = g_P = 0$.

The Hamiltonian in the presence of only scalar and tensor operators can be written as,

$$\begin{aligned}\mathcal{H}_{\text{eff}} = \frac{G_F V_{qq'}}{\sqrt{2}}[\bar{l}(1-\gamma_5)\nu_l \bar{q}'(A_S + B_S\gamma_5)q \\ + T_L \bar{l}\sigma_{\mu\nu}(1-\gamma_5)\nu_l \bar{q}'\sigma^{\mu\nu}(1-\gamma_5)q],\end{aligned} \tag{4}$$

where $A_S = S_R + S_L$ and $B_S = S_R - S_L$ with S_L and S_R are the left- and right-handed scalar couplings and T_L is the tensor coupling.

We will first employ a model independent approach and treat the scalar and tensors coupling one at a time. Since, in many realistic models both the scalar and tensor couplings may be present, we will consider an explicit leptoquark model where both the scalar and tensor couplings are present.

The Hamiltonian in the presence of only $V \pm A$ operators was considered in our previous work [12]. There the effective Hamiltonian was written in terms of a W' model, which could arise in extensions of the SM [15], as

$$\mathcal{L} = \frac{g}{\sqrt{2}} V_{f'f} \bar{f}'\gamma^\mu (g_L^{f'f} P_L + g_R^{f'f} P_R) f W'_\mu + \text{H.c.} \tag{5}$$

Integrating out the W' leads to

$$\begin{aligned}\mathcal{L} &= \frac{g^2}{2M_W^2} V_{f'f}\left[\bar{f}'\gamma^\mu\left(\frac{M_W^2}{M_{W'}^2} g_L^{f'f} P_L + \frac{M_W^2}{M_{W'}^2} g_R^{f'f} P_R\right) f\right] \\ &\quad \times [g^{l,\nu_l}\bar{l}\gamma_\mu P_L \nu_l] + \text{H.c.}, \\ \mathcal{L} &= \frac{4G_F V_{f'f}}{\sqrt{2}}\left[\bar{f}'\gamma^\mu\left(\frac{M_W^2}{M_{W'}^2} g_L^{f'f} P_L + \frac{M_W^2}{M_{W'}^2} g_R^{f'f} P_R\right) f\right] \\ &\quad \times [g_{\nu_l,l}\bar{l}\gamma_\mu P_L \nu_l] + \text{H.c.}\end{aligned} \tag{6}$$

Comparing Eq. (6) with Eq. (3) we have the following relations

$$\begin{aligned}V_L &= \frac{M_W^2}{M_{W'}^2} g_L^{f'f} g^{l,\nu_l}, \\ V_R &= \frac{M_W^2}{M_{W'}^2} g_R^{f'f} g^{l,\nu_l}.\end{aligned} \tag{7}$$

A. Deep inelastic neutrino nucleon scattering

In this section we discuss deep inelastic neutrino nucleon scattering with the various types of interactions.

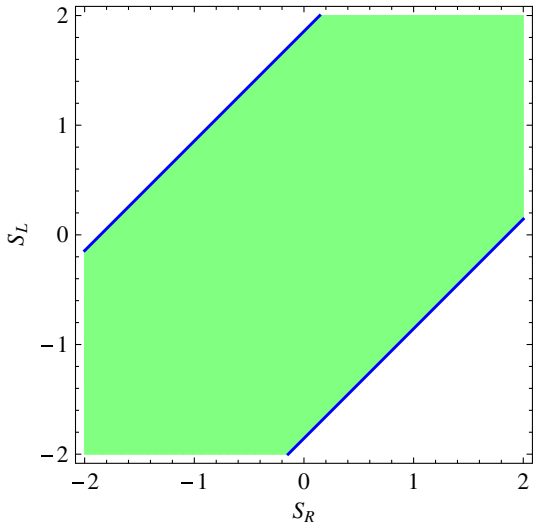

FIG. 1 (color online). The constraints on the scalar couplings $S_{L,R}$. The colored region is allowed. The constraint is from $\tau^- \to \pi^- \nu_\tau$. We treat S_L and S_R as real couplings.

1. Scalar and tensor interactions

In this section, we first present the total and differential cross sections for the deep inelastic scattering (DIS) process

$$\nu_\tau + N \to \tau + X, \qquad \nu_\mu + N \to \mu + X, \tag{8}$$

with scalar and tensor interactions. The total differential cross section is written in terms of contributions from the standard model, scalar and tensor operators and cross terms as follows

$$\frac{d\sigma_{\rm tot}}{dxdy} = \frac{d\sigma_{\rm SM}}{dxdy} + \frac{d\sigma_{\rm LQS}}{dxdy} + \frac{d\sigma_{\rm LQT}}{dxdy} + \frac{d\sigma_{\rm SM,LQ}}{dxdy} + \frac{d\sigma_{\rm LQS,LQT}}{dxdy}. \tag{9}$$

The differential cross section is given in terms of the cross section amplitude as follows

$$\frac{d\sigma}{dxdy} = \frac{1}{32\pi M E_\nu} \int \frac{d\xi}{\xi} f(\xi) |\bar{\mathcal{M}}(\xi)|^2 \delta(\xi - x). \tag{10}$$

Here, $p_q^\mu = \xi p^\mu$ is the four-momentum of the scattered quark, p^μ is the target nucleon, and ξ is its momentum fraction. $f(\xi)$ is the parton distribution function (PDF) inside a nucleon and E_ν is the incoming neutrino energy. In the deep inelastic scattering we calculate the differential cross section with respect to the scaling variables which are defined as follows

$$x = \frac{q^2}{2\nu}, \qquad y = \frac{\nu}{M E_\nu}, \tag{11}$$

where x is the Bjorken variable and y is the inelasticity with q being the four-momentum transfer of the leptonic probe and

$$\nu = -p \cdot q = M(E_\nu - E_\ell). \tag{12}$$

The physical regions for x and y are obtained by Albright and Jarlskog [16,17]

$$\frac{m_\ell^2}{2M(E_\nu - m_\ell)} \le x \le 1, \tag{13}$$

and

$$A - B \le y \le A + B, \tag{14}$$

where

$$A = \frac{1}{2}\left(1 - \frac{m_\ell^2}{2ME_\nu x} - \frac{m_\ell^2}{2E_\nu^2}\right) \Big/ \left(1 + \frac{xM}{2E_\nu}\right), \tag{15}$$

$$B = \frac{1}{2}\left[\left(1 - \frac{m_\ell^2}{2ME_\nu x}\right)^2 - \frac{m_\ell^2}{E_\nu^2}\right]^{\frac{1}{2}} \Big/ \left(1 + \frac{xM}{2E_\nu}\right). \tag{16}$$

The terms in Eq. (9) are given as

$$\begin{aligned}
\frac{d\sigma_{\rm SM}}{dxdy} &= \frac{G_F^2 M E_\nu}{\pi}\left(y\left(xy + \frac{m_\ell^2}{2ME_\nu}\right)F_1 \right. \\
&\quad + \left(1 - y - \frac{Mxy}{2E_\nu} - \frac{m_\ell^2}{4E_\nu^2}\right)F_2 \\
&\quad \left. + \left(xy\left(1 - \frac{y}{2}\right) - y\frac{m_\ell^2}{4ME_\nu}\right)F_3 - \frac{m_\ell^2}{2ME_\nu}F_5\right), \\
\frac{d\sigma_{\rm LQS}}{dxdy} &= \frac{G_F^2 M E_\nu}{4\pi}(A_S^2 + B_S^2) y\left(xy + \frac{m_\ell^2}{2ME_\nu}\right)F_1, \\
\frac{d\sigma_{\rm LQT}}{dxdy} &= \frac{8G_F^2 M E_\nu}{\pi} T_L^2 \left(y\left(xy + \frac{m_\ell^2}{2ME_\nu}\right)F_1 \right. \\
&\quad \left. + 2\left(1 - y - \frac{Mxy}{4E_\nu} - \frac{m_\ell^2}{8E_\nu^2}\right)F_2 - \frac{m_\ell^2}{ME_\nu}F_5\right), \\
\frac{d\sigma_{\rm SM,LQ}}{dxdy} &= 0, \\
\frac{d\sigma_{\rm LQS,LQT}}{dxdy} &= \frac{2G_F^2 M E_\nu}{\pi} T_L (B_S - A_S) \\
&\quad \times \left(xy\left(1 - \frac{y}{2}\right) - y\frac{m_\ell^2}{4ME_\nu}\right)F_3.
\end{aligned} \tag{17}$$

The functions F_i are given as

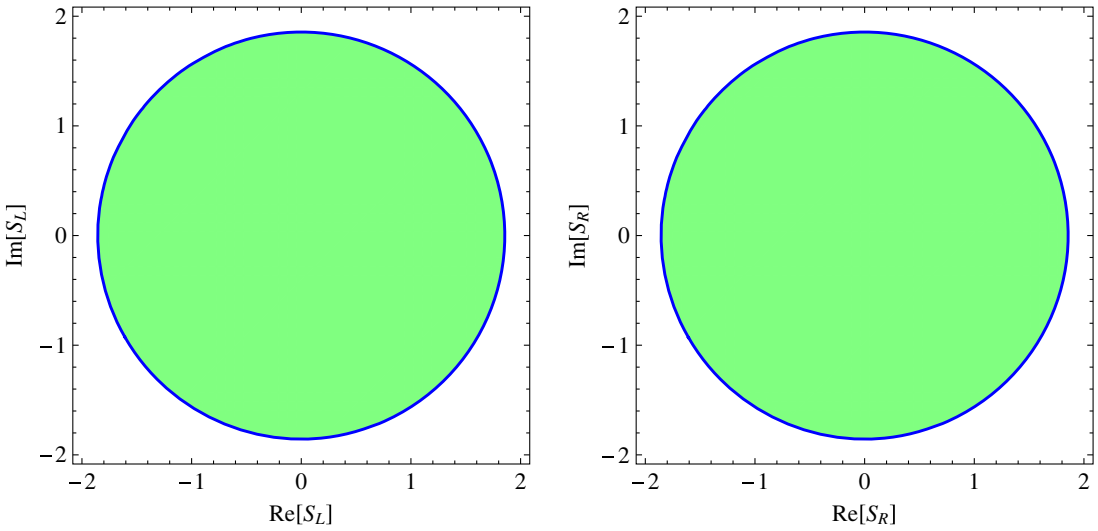

FIG. 2 (color online). The constraints on the scalar couplings $S_{L,R}$. The colored region is allowed. The constraint is from $\tau^- \to \pi^- \nu_\tau$. Left panel: we take $S_R = 0$ and treat S_L as a complex coupling. Right panel: we take $S_L = 0$ and treat S_R as a complex coupling.

$$
\begin{aligned}
F_1 &= \sum_{q,\bar{q}} f_{q,\bar{q}}(\xi, Q^2) V_{q,q'}^2, \\
F_2 &= 2\sum_{q,\bar{q}} \xi f_{q,\bar{q}}(\xi, Q^2) V_{q,q'}^2, \\
F_3 &= 2\sum_{q} f_{q}(\xi, Q^2) V_{q,q'}^2 - 2\sum_{\bar{q}} f_{\bar{q}}(\xi, Q^2) V_{\bar{q},\bar{q}'}^2, \\
F_5 &= 2\sum_{q,\bar{q}} f_{q,\bar{q}}(\xi, Q^2) V_{q,q'}^2,
\end{aligned} \tag{18}
$$

where f_q and $f_{\bar{q}}$ are the parton distribution functions inside a nucleon, $V_{q,q'}$ is the CKM matrix element, and $Q^2 = -q^2$.

One can write the differential cross sections above in terms of different variables (t, ν) using Eq. (11) and the transformation [17],

$$
\frac{d\sigma}{dxdy} = 2ME_\nu \nu \frac{d\sigma}{dq^2 d\nu}. \tag{19}
$$

In the new variables, the differential cross sections can be written in the form

$$
\begin{aligned}
\frac{d\sigma_{\rm SM}}{dq^2 d\nu} &= \frac{G_F^2}{8\pi M E_\nu^2}\left(2(q^2 + m_\ell^2)W_1 + \left(4E_\nu\left(E_\nu - \frac{\nu}{M}\right) - (q^2 + m_\ell^2)\right)W_2 \right. \\
&\quad \left. + \frac{1}{M^2}(2ME_\nu q^2 - \nu(q^2 + m_\ell^2))W_3 - \frac{2m_\ell^2 E_\nu}{M} W_5\right), \\
\frac{d\sigma_{\rm LQS}}{dq^2 d\nu} &= \frac{G_F^2}{16\pi M E_\nu^2}(A_S^2 + B_S^2)(m_\ell^2 + q^2)W_1, \\
\frac{d\sigma_{\rm LQT}}{dq^2 d\nu} &= \frac{G_F^2}{\pi M E_\nu^2} T_L^2 \left(2(m_\ell^2 + q^2)W_1 + \left(8E_\nu^2 - (m_\ell^2 + q^2) - \frac{8E_\nu \nu}{M}\right)W_2 - \frac{4m_\ell^2 E_\nu}{M} W_5\right), \\
\frac{d\sigma_{\rm LQS,LQT}}{dq^2 d\nu} &= \frac{G_F^2}{4\pi M^3 E_\nu^2} T_L (B_S - A_S)(2E_\nu M q^2 - (m_\ell^2 + q^2)\nu)W_3,
\end{aligned} \tag{20}
$$

where the (time-reversal invariant) structure functions are [17]

$$
\begin{aligned}
W_1(q^2, \nu) &= \frac{F_1(x)}{M}, \qquad W_2(q^2, \nu) = \frac{MF_2(x)}{\nu}, \\
W_3(q^2, \nu) &= \frac{MF_3(x)}{\nu}, \qquad W_5(q^2, \nu) = \frac{MF_5(x)}{\nu}.
\end{aligned} \tag{21}
$$

We also define some Lorentz invariant variables in terms of the four-momenta of incoming neutrino (k), target nucleon (p), and produced charged lepton (k') in the laboratory frame

$$
Q^2 = -q^2 = -t, \tag{22}
$$

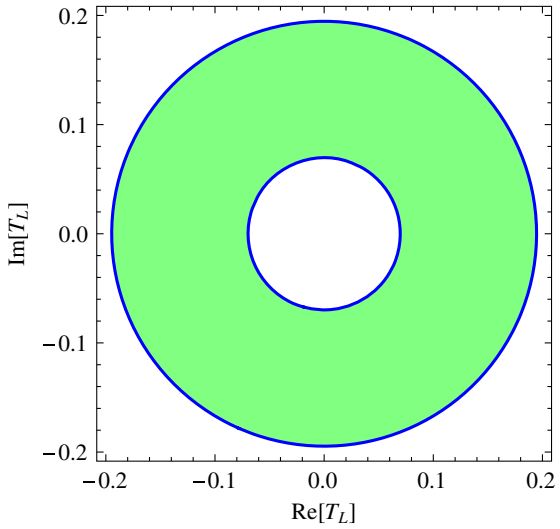

FIG. 3 (color online). The allowed region for the real and imaginary components of the complex leptoquark coupling T_L. The constraint on T_L is from $\tau^- \to \pi^-\pi^0\nu_\tau$.

$$W^2 = (p+q)^2. \tag{23}$$

Q^2 is the magnitude of the momentum transfer and W is the hadronic invariant mass. The physical regions of these variables are given by [18]

$$W_{\rm cut} \le W \le \sqrt{s} - m_\ell, \tag{24}$$

in the DIS region with $W_{\rm cut} = 1.4$–1.6 GeV, and

$$Q^2_-(W) \le Q^2 \le Q^2_+(W), \tag{25}$$

where $s = (k+p)^2$ and

$$Q^2_\pm(W) = \frac{s-M^2}{2}(1 \pm \bar\beta) - \frac{1}{2}\left[W^2 + m_\ell^2 - \frac{M^2}{s}(W^2 - m_\ell^2)\right], \tag{26}$$

with $\bar\beta = \lambda^{\frac{1}{2}}(1, m_\ell^2/s, W^2/s)$ and $\lambda(a,b,c) = a^2 + b^2 + c^2 - 2(ab+bc+ca)$. In the lab frame, $s = M^2 + 2ME_\nu$.

2. Explicit leptoquark model

Here we will discuss an explicit leptoquark model. Many extensions of the SM, motivated by a unified description of quarks and leptons, predict the existence of new scalar and vector bosons, called leptoquarks, which decay into a quark and a lepton. These particles carry nonzero baryon and lepton numbers, color, and fractional electric charges. The most general dimension four $SU(3)_c \times SU(2)_L \times U(1)_Y$ invariant Lagrangian of leptoquarks satisfying baryon and lepton number conservation was considered in Ref. [19]. As the tensor operators in the effective Lagrangian get contributions only from scalar leptoquarks, we will focus only on scalar leptoquarks and consider the case where the leptoquark is a weak doublet or a weak singlet. The weak doublet leptoquark, R_2 has the quantum numbers $(3, 2, -7/6)$ under $SU(3)_c \times SU(2)_L \times U(1)_Y$ while the singlet leptoquark S_1 has the quantum numbers $(\bar 3, 1, -1/3)$.

The interaction Lagrangian that induces contributions to $\nu_\tau + N \to \tau + X$ process is [20,21]

$$\begin{aligned}\mathcal{L}_2^{\rm LQ} &= (g_{2L}^{ij}\bar u_{iR} L_{jL} + g_{2R}^{ij}\bar Q_{jL} i\sigma_2 l_{iR})R_2,\\ \mathcal{L}_0^{\rm LQ} &= (g_{1L}^{ij}, \bar Q_{iL}^c i\sigma_2 L_{jL} + g_{1R}^{ij}, \bar u_{iR}^c \ell_{jR})S_1,\end{aligned} \tag{27}$$

where Q_i and L_j are the left-handed quark and lepton $SU(2)_L$ doublets, respectively, while u_{iR}, d_{iR}, and ℓ_{jR} are

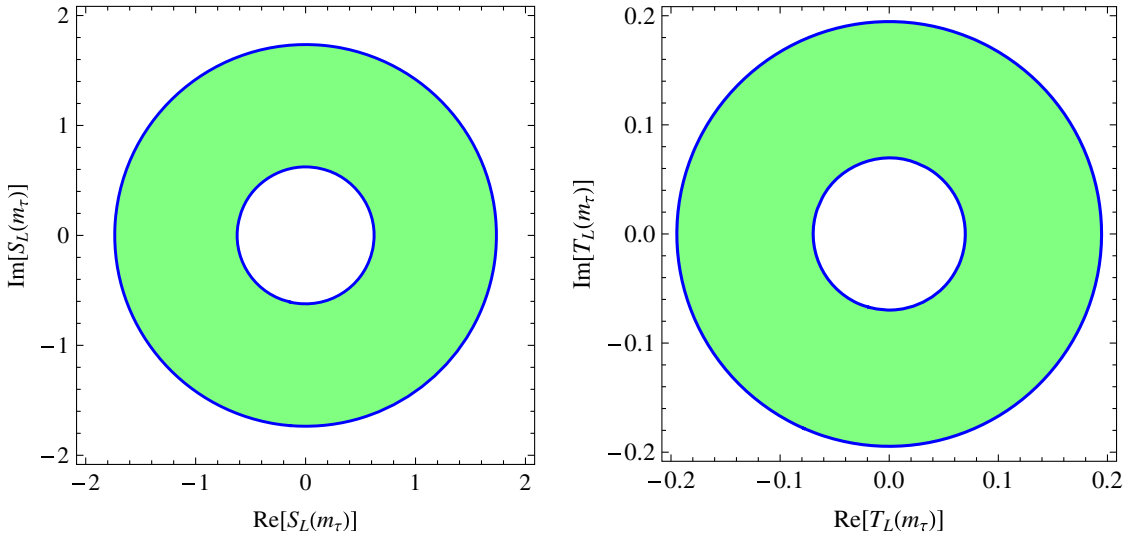

FIG. 4 (color online). The allowed regions for the real and imaginary components of the leptoquark running couplings $S_L(m_\tau)$ and $T_L(m_\tau)$ with $S_L(m_{LQ}) = \pm 4 T_L(m_{LQ})$ at $m_{\rm LQ} = 1000$ GeV. The constraint on $S_L(m_\tau)$ is from $\tau^- \to \pi^-\nu_\tau$ and $T_L(m_\tau)$ is from $\tau^- \to \pi^-\pi^0\nu_\tau$.

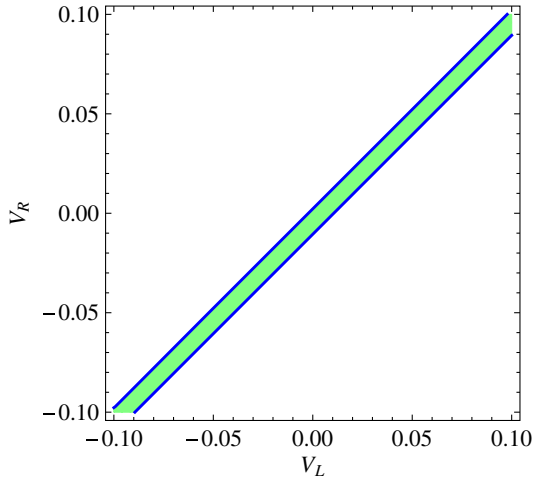

FIG. 5 (color online). The allowed regions for the left- and right-handed couplings V_L and V_R. The constraint are from $\tau^- \to \pi^-\nu_\tau$ and $\tau^- \to \pi^-\pi^0\nu_\tau$.

the right-handed up, down quark and charged lepton $SU(2)_L$ singlets. Indices i and j denote the generations of quarks and leptons and $\psi^c = C\bar{\psi}^T = C\gamma^0\psi^*$ is a charge-conjugated fermion field. The fermion fields are given in the gauge eigenstate basis and one should make the transformation to the mass basis. Assuming the quark mixing matrices to be hierarchical, and considering only the leading contribution we can ignore the effect of mixing.

The couplings in Eq. (27) can be constrained from τ decays. Because of the doublet nature of R_2 there will be additional term like $\bar{\tau}\tau\bar{q}q$ which do not contribute to τ decays. They will contribute to tau pair production but are much smaller than the SM production and hence do not add any new constraints.

After performing the Fierz transformations, one finds the general Wilson coefficients at the leptoquark mass scale contributing to the $\nu_\tau + N \to \tau + X$ process:

$$S_L = \frac{1}{2\sqrt{2}G_F V_{ud}}\left[-\frac{g_{1L}^{13}g_{1R}^{13*}}{2M_{S_1}^2} - \frac{g_{2L}^{13}g_{2R}^{13*}}{2M_{R_2}^2}\right],$$
$$T_L = \frac{1}{2\sqrt{2}G_F V_{ud}}\left[\frac{g_{1L}^{13}g_{1R}^{13*}}{8M_{S_1}^2} - \frac{g_{2L}^{13}g_{2R}^{13*}}{8M_{R_2}^2}\right]. \quad (28)$$

It is clear from Eq. (28) that the weak singlet leptoquark and the weak doublet can add constructively or destructively to the Wilson's coefficients of the scalar and tensor operators in the effective Hamiltonian. In this section we will also consider the possibilities where both the scalar and the tensor operators are present and are of similar sizes. In the most general case both the singlet and doublet leptoquarks are present and so both the scalar and tensor operators appear in the effective Hamiltonian. As there is limited experimental information, including both the singlet and the doublet leptoquarks will allow us more flexibility in fitting for the Wilson's coefficients but this will come with the price of less precise predictions for the various observables. We can, therefore, consider the simpler cases when only a singlet or a doublet leptoquark are present. In these cases, from Eq. (28) the coefficients of scalar operators and the tensor operators have the same magnitudes. One can then consider the two cases:

Case (i): In this case only the weak doublet scalar leptoquark R_2 is present. In this case the Wilson's coefficients are

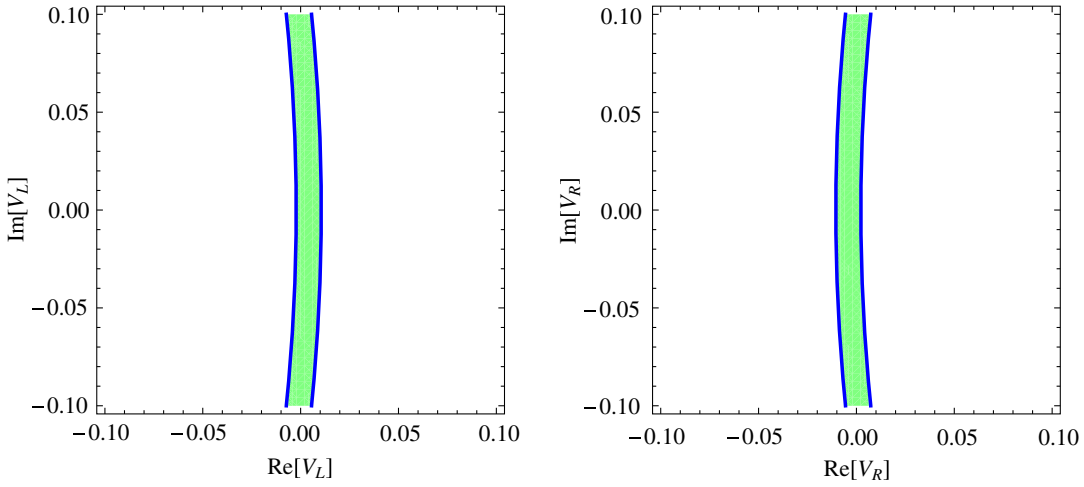

FIG. 6 (color online). The allowed regions for the left- and right-handed complex couplings V_L and V_R. The constraint are from $\tau^- \to \pi^-\nu_\tau$ and $\tau^- \to \pi^-\pi^0\nu_\tau$. Left panel: we take $V_R = 0$ and treat V_L as a complex coupling. Right panel: we take $V_L = 0$ and treat V_R as a complex coupling.

$$S_L = \frac{1}{2\sqrt{2}G_F V_{cb}}\left[-\frac{g_{2L}^{13} g_{2R}^{13*}}{2M_{R_2}^2}\right],$$
$$T_L = \frac{1}{2\sqrt{2}G_F V_{cb}}\left[-\frac{g_{2L}^{13} g_{2R}^{13*}}{8M_{R_2}^2}\right], \quad (29)$$

Case (ii): In this case only the singlet leptoquark is present and the relevant Wilson's coefficients are

$$S_L = \frac{1}{2\sqrt{2}G_F V_{cb}}\left[-\frac{g_{1L}^{33} g_{1R}^{23*}}{2M_{S_1}^2}\right],$$
$$T_L = \frac{1}{2\sqrt{2}G_F V_{cb}}\left[\frac{g_{1L}^{33} g_{1R}^{23*}}{8M_{S_1}^2}\right]. \quad (30)$$

In the $(\bar{3}, 1, -1/3)$ case proton decay can occur in presence of an additional leptoquark couplings to two quarks. The proton decay only constraints the leptoquark mass and the product of this additional coupling with the coupling considered here and so we can choose to turn the proton decay constraint as a constraint on the additional coupling involving the two quarks. Moreover, the relevant couplings for the considered processes involve the third generation and so proton decay constraints do not apply in general to these couplings. Also note the proton cannot kinematically decay to a τ.

The relations in Eqs. (29), (30) are valid at the leptoquark mass scale. We have to run them down to the τ mass scale using the scale dependence of the scalar and tensor currents at leading logarithm approximation

$$S_L(m_\tau) = \left[\frac{\alpha_s(m_t)}{\alpha_s(m_\tau)}\right]^{\frac{\gamma_S}{2\beta_0^{(5)}}}\left[\frac{\alpha_s(m_{\rm LQ})}{\alpha_s(m_t)}\right]^{\frac{\gamma_S}{2\beta_0^{(6)}}} S_L(m_{\rm LQ}),$$
$$T_L(m_\tau) = \left[\frac{\alpha_s(m_t)}{\alpha_s(m_\tau)}\right]^{\frac{\gamma_T}{2\beta_0^{(5)}}}\left[\frac{\alpha_s(m_{\rm LQ})}{\alpha_s(m_t)}\right]^{\frac{\gamma_T}{2\beta_0^{(6)}}} T_L(m_{\rm LQ}), \quad (31)$$

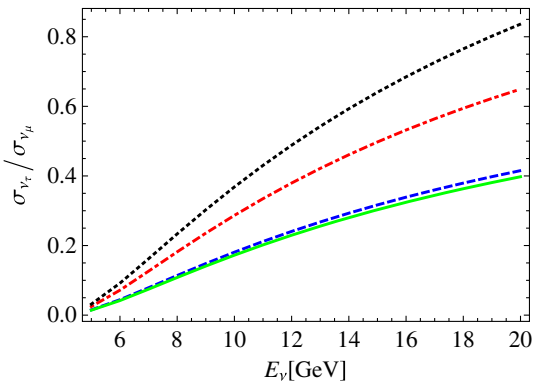

FIG. 7 (color online). $S \pm T$ model: The ratio between the total cross section of $\nu_\tau + N \to \tau + X$ to $\nu_\mu + N \to \mu + X$ with scalar-tensor couplings. The green solid line corresponds to the standard model prediction $S_R = S_L = T_L = 0$. The blue dashed, red dot dashed and black dotted lines correspond to $(S_R, S_L, T_L) = (-0.19, 0.68, 0.072)$, $(1.98, 0.42, -0.13)$, $(-1.87, -1.31, 0.18)$.

where the anomalous dimensions of the scalar and tensor operators are $\gamma_S = -6C_F = -8$, $\gamma_T = 2C_F = 8/3$, respectively. Further, the beta function, $\beta_0^{(f)} = 11 - 2n_f/3$ [22–24] and n_f is a number of active quark flavors. One can use the equations above to run down couplings from a chosen value of $m_{\rm LQ}$ to the tau mass, m_τ.

In the presence of only one type of leptoquark, singlet or tensor state, one finds that the scalar S_L and tensor T_L Wilson coefficients are related to each other at the scale of leptoquark mass, $S_L(m_{\rm LQ}) = \pm 4T_L(m_{\rm LQ})$.

3. $V \pm A$ interactions

The DIS differential cross section in the presence of V ± A operators with respect to the variables (x, y) is given in [12]. Here we write it in terms of the momentum transfer, using Eq. (19) as follows

$$\frac{d\sigma_{\rm SM+(V\pm A)}}{dq^2 d\nu} = \frac{G_F^2}{8\pi M E_\nu^2}((|a'|^2 + |b'|^2)(m_\ell^2 + q^2)W_1$$
$$+ \frac{1}{2M}(|a'|^2 + |b'|^2)(4E_\nu^2 M - 4E_\nu \nu$$
$$- M(m_\ell^2 + q^2))W_2$$
$$+ \frac{1}{M^2}{\rm Re}[a'b'^*](2E_\nu M q^2 - \nu(m_\ell^2 + q^2))W_3$$
$$- \frac{1}{M}(|a'|^2 + |b'|^2)m_\ell^2 E_\nu W_5), \quad (32)$$

where the definitions are

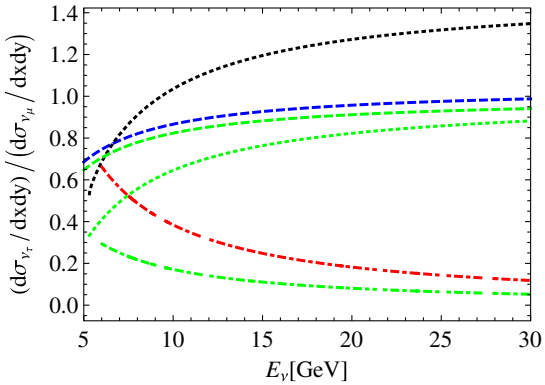

FIG. 8 (color online). $S \pm T$ model: The ratio between the differential cross section $(d\sigma/dxdy)$ of $\nu_\tau + N \to \tau + X$ to $\nu_\mu + N \to \mu + X$ with scalar-tensor couplings. The green lines correspond to the standard model predictions with $S_R = S_L = T_L = 0$. The blue, black, and red lines correspond to $(S_R, S_L, T_L) = (-0.19, 0.68, 0.072)$, $(1.98, 0.42, -0.13)$, $(-1.87, -1.31, 0.18)$. The blue and green dashed lines correspond to $(x, y) = (0.95, A + B)$. The black and green dot dashed lines correspond to $(x, y) = (0.475, (A + B)/2)$. The red and green dotted lines correspond to $(x, y) = (\frac{m_\tau^2}{2M(E_\nu - m_\tau)}, A - B)$.

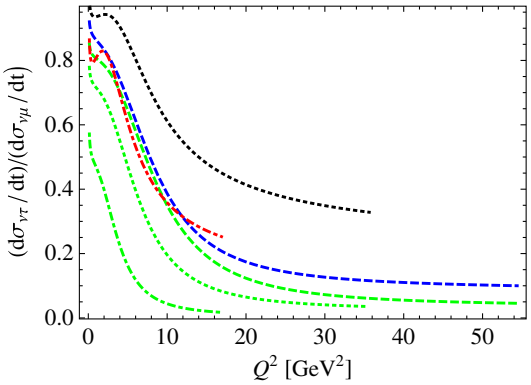

FIG. 9 (color online). $S \pm T$ model: The ratio between the differential cross section $(d\sigma/dt)$ of $\nu_\tau + N \to \tau + X$ to $\nu_\mu + N \to \mu + X$ in the scalar-tensor model. The green dashed, dotted and dotdashed lines correspond to the standard model predictions with $S_R = S_L = T_L = 0$ at $E_\nu = 30$, 20, 10, respectively. The blue dashed, black dotted, and red dot dashed lines correspond to $(S_R, S_L, T_L) = (-0.19, 0.68, 0.072)$, $(1.98, 0.42, -0.13)$, $(-1.87, -1.31, 0.18)$ at $E_\nu = 30$, 20, 10, respectively. The physical regions of the momentum transfer taken to be $Q^2_-(W_{\rm cut}) \le Q^2 \le Q^2_+(W_{\rm cut})$.

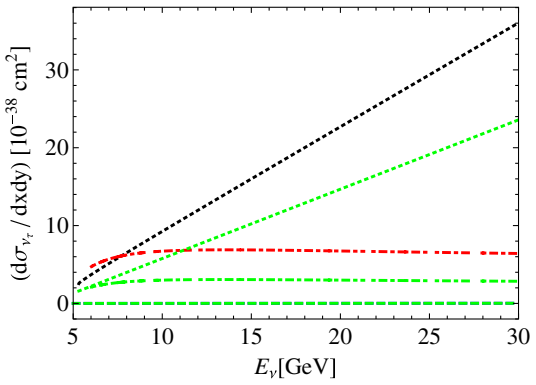

FIG. 11 (color online). $S \pm T$ model: The differential cross section $(d\sigma/dxdy)$ of $\nu_\tau + N \to \tau + X$ in the scalar-tensor model. The green lines correspond to the standard model predictions with $S_R = S_L = T_L = 0$. The blue, black, and red lines correspond to $(S_R, S_L, T_L) = (-0.19, 0.68, 0.072)$, $(1.98, 0.42, -0.13)$, $(-1.87, -1.31, 0.18)$. The blue and green dashed lines correspond to $(x, y) = (0.95, A + B)$. The black and green dot dashed lines correspond to $(x, y) = (0.475, (A + B)/2)$. The red and green dotted lines correspond to $(x, y) = (\frac{m_\tau^2}{2M(E_\nu - m_\tau)}, A - B)$.

$$
\begin{aligned}
a' &= 1 + \gamma^\rho, \\
b' &= 1 + \gamma^\kappa, \\
\gamma^\rho &= V_L + V_R, \\
\gamma^\kappa &= V_L - V_R.
\end{aligned} \tag{33}
$$

III. CONSTRAINTS ON NP COUPLINGS

The scalar couplings S_L and S_R can be constrained by the tau decay channel $\tau^-(k_1) \to \nu_\tau(k_2) + \pi^-(q)$, while the tensor coupling T_L can be constrained by the three-body decay channel $\tau(p) \to \pi^-(p_1) + \pi^0(p_2) + \nu_\tau(p_3)$. In this section we will discuss the constraints.

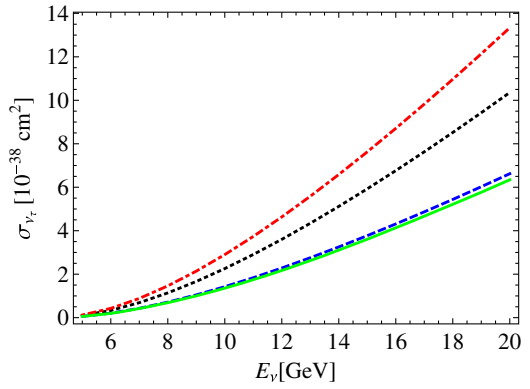

FIG. 10 (color online). $S \pm T$ model: The total cross section of $\nu_\tau + N \to \tau + X$ in the scalar-tensor model. The green solid line corresponds to the standard model prediction $S_R = S_L = T_L = 0$. The blue dashed, black dotted and red dot dashed lines correspond to $(S_R, S_L, T_L) = (-0.19, 0.68, 0.072)$, $(1.98, 0.42, -0.13)$, $(-1.87, -1.31, 0.18)$.

A. $\tau^-(k_1) \to \nu_\tau(k_2) + \pi^-(q)$

The hadronic current of the bound state π can be parametrized as

$$\langle 0|\bar{d}\gamma^\mu(1-\gamma^5)u|\pi(q)\rangle = -i\sqrt{2}f_\pi q^\mu, \tag{34}$$

where $f_\pi = (92.4 \pm 0.1 \pm 0.3)$ MeV [25] is the decay constant. The SM decay rate is

$$\Gamma^\pi_{\rm SM} = \frac{1}{8\pi} G_F^2 |V_{ud}|^2 f_\pi^2 m_\tau^3 \left(1 - \frac{m_\pi^2}{m_\tau^2}\right)^2 \delta_{\tau/\pi}. \tag{35}$$

Here $\delta_{\tau/\pi} = 1.0016 \pm 0.0014$ [26] is the radiative correction. Further, the SM branching ratio can also be expressed as [27]

$$\mathrm{Br}^{\rm SM}_{\tau^- \to \pi^- \nu_\tau} = 0.607 \mathrm{Br}(\tau^- \to \nu_\tau e^- \bar{\nu}_e) = 10.82 \pm 0.02\%, \tag{36}$$

while the measured $\mathrm{Br}(\tau^- \to \pi^- \nu_\tau)_{\rm exp} = (10.91 \pm 0.07)\%$ [25]. In the presence of a scalar state, the decay rate is

$$\Gamma^\pi_S = \frac{1}{8\pi} G_F^2 |V_{ud}|^2 B_S^2 f_\pi^2 m_\pi^2 m_\tau \left(1 - \frac{m_\pi^2}{m_\tau^2}\right)^2, \tag{37}$$

where

$$\langle 0|\bar{d}(A_S - B_S\gamma^5)u|\pi(q)\rangle = i\sqrt{2}f_\pi m_\pi B_S. \tag{38}$$

In order to obtain the scalar hadronic current above, we have multiplied the SM hadronic current (34) by the sum and difference of the quark momenta and used the equation

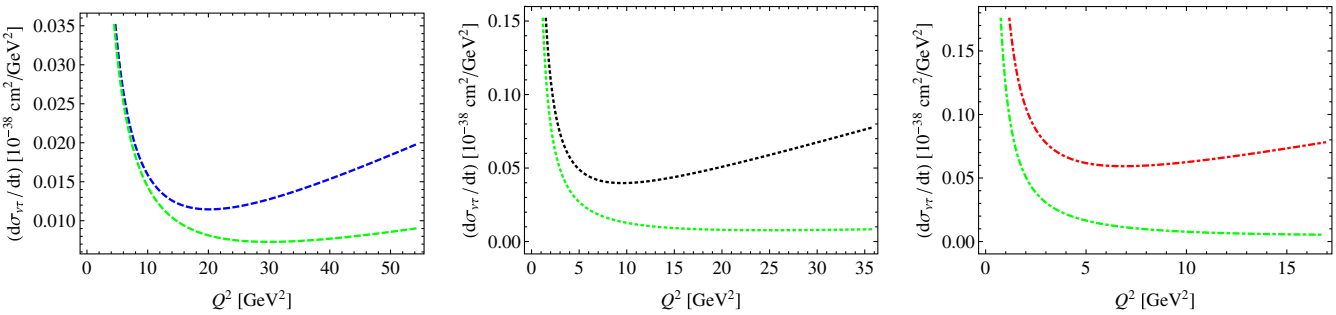

FIG. 12 (color online). $S \pm T$ model: The differential cross section $(d\sigma/dt)$ of $\nu_\tau + N \to \tau + X$ in the scalar-tensor model. The green dashed, dotted and dot dashed lines correspond to the standard model predictions with $S_R = S_L = T_L = 0$ at $E_\nu = 30$ (left), 20 (middle) and 10 (right), respectively. The blue dashed, black dotted, and red dot dashed lines correspond to $(S_R, S_L, T_L) = (-0.19, 0.68, 0.072)$, $(1.98, 0.42, -0.13)$, $(-1.87, -1.31, 0.18)$ at $E_\nu = 30$, 20, 10, respectively. The physical regions of the momentum transfer taken to be $Q^2_-(W_{\rm cut}) \le Q^2 \le Q^2_+(W_{\rm cut})$.

of motion—see Appendix (B). The total branching ratio can be written as follows

$$\mathrm{BR}^\pi_{\rm tot} = \mathrm{BR}^\pi_{\rm SM}(1 + (r^\pi_{\rm S})^2), \tag{39}$$

where

$$(r^\pi_{\rm S})^2 = \frac{\mathrm{BR}^\pi_{\rm S}}{\mathrm{BR}^\pi_{\rm SM}}, \tag{40}$$

with

$$r^\pi_{\rm S} = \frac{B_S m_\pi}{m_\tau}. \tag{41}$$

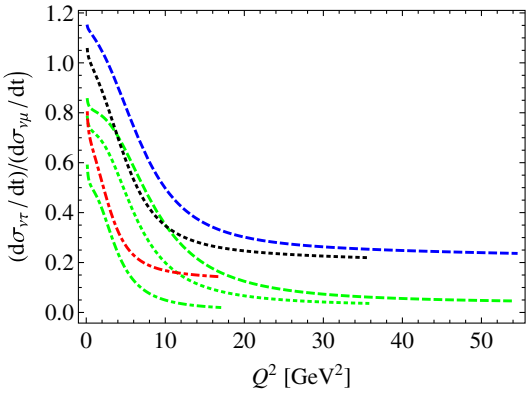

FIG. 13 (color online). Leptoquark: The ratio between the differential cross section $(d\sigma/dt)$ of $\nu_\tau + N \to \tau + X$ to $\nu_\mu + N \to \mu + X$ in the leptoquark model with $S_L(m_{\rm LQ}) = \pm 4T_L(m_{\rm LQ})$ at $m_{\rm LQ} = 1000$ GeV. The green dashed, dotted and dot dashed lines correspond to the standard model predictions with $S_R = S_L = T_L = 0$ at $E_\nu = 30$, 20, 10, respectively. The blue, black, and red lines correspond to $(\mathrm{Re}[S_L(m_{\rm LQ})], \mathrm{Im}[S_L(m_{\rm LQ})], \mathrm{Re}[T_L(m_{\rm LQ})], \mathrm{Im}[T_L(m_{\rm LQ})]) = (0.56, 0.60, 0.14, 0.15)$ at $E_\nu = 30$, 20, 10, respectively. The physical regions of the momentum transfer taken to be $Q^2_-(W_{\rm cut}) \le Q^2 \le Q^2_+(W_{\rm cut})$.

Note, the interference term of the SM and the scalar NP term vanishes.

The allowed region of the couplings are given in the contour plot Fig. 1 for the measured $\tau^- \to \pi^- \nu_\tau$ within the 2σ level. First, we assume both couplings, $S_{L,R}$, are present and take the couplings to be real. Next we assume the couplings are complex and take one coupling at a time, see Fig. 2.

B. $\tau(p) \to \pi^-(p_1) + \pi^0(p_2) + \nu_\tau(p_3)$

Here we consider two-pion decays of τ. The process is

$$\tau(p) \to \nu_\tau(p_3) + \pi^-(p_1) + \pi^0(p_2). \tag{42}$$

The SM and NP amplitudes are

$$M_{\rm SM} = \frac{-iG_F V_{ud}}{\sqrt{2}} \langle \pi^-\pi^0 | \bar{d}\gamma^\mu (1-\gamma^5) u | 0 \rangle \bar{u}_{\nu_\tau} \gamma_\mu (1-\gamma^5) u_\tau, \tag{43}$$

$$M_T = \frac{G_F V_{ud}}{\sqrt{2}} T_L \langle \pi^-\pi^0 | \bar{d}\sigma^{\mu\nu} (1-\gamma^5) u | 0 \rangle \bar{u}_{\nu_\tau} \sigma_{\mu\nu} (1-\gamma^5) u_\tau. \tag{44}$$

We can parametrize the relevant form factors as,

$$\langle \pi^-\pi^0 | \bar{d}\gamma^\mu (1-\gamma^5) u | 0 \rangle = \sqrt{2} F(Q^2) k^\mu, \tag{45}$$

$$\langle \pi^-\pi^0 | \bar{d}\sigma^{\mu\nu} (1-\gamma^5) u | 0 \rangle = \sqrt{2} F_T(Q^2)(k^\mu q^\nu - q^\mu k^\nu), \tag{46}$$

where $k = p_1 - p_2$ and $q = p_1 + p_2$. The form factor $F(Q^2)$, along with its error, is given in [28,29]. In our analysis, errors of the form factor parameters have been considered and included in the constraint plots. The origin of $\sqrt{2}$ comes from the wave function of $\pi^0 = \frac{1}{\sqrt{2}}(u\bar{u} + d\bar{d})$. Considering the isospin symmetry, $u\bar{u} = d\bar{d} = \phi$, so $\pi^0 = \sqrt{2}\phi$. Using the equations of motion and by

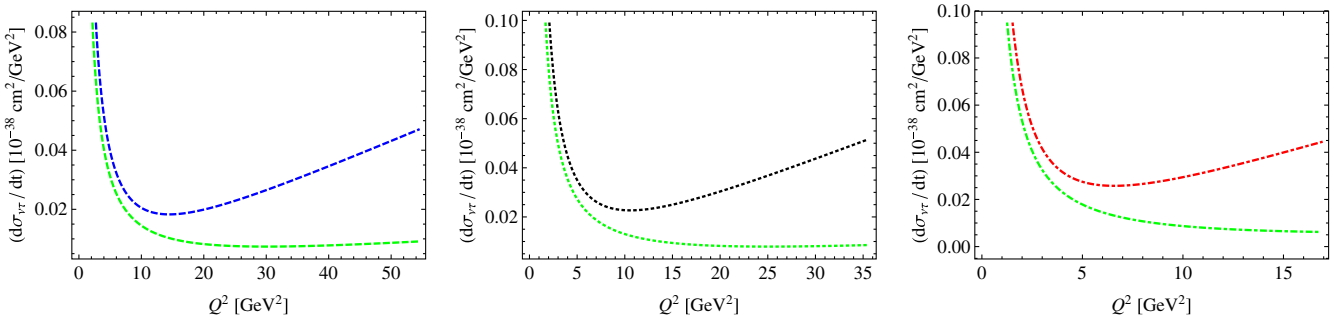

FIG. 14 (color online). Leptoquark: The differential cross section $(d\sigma/dt)$ of $\nu_\tau + N \to \tau + X$ in the leptoquark model with $S_L(m_{\rm LQ}) = \pm 4T_L(m_{\rm LQ})$ at $m_{\rm LQ} = 1000$ GeV. The green dashed, dotted and dot dashed lines correspond to the standard model predictions with $S_R = S_L = T_L = 0$ at $E_\nu = 30$ (left), 20 (middle) and 10 (right), respectively. The blue, black, and red lines correspond to $(\mathrm{Re}[S_L(m_{\rm LQ})], \mathrm{Im}[S_L(m_{\rm LQ})], \mathrm{Re}[T_L(m_{\rm LQ})], \mathrm{Im}[T_L(m_{\rm LQ})]) = (0.56, 0.60, 0.14, 0.15)$ at $E_\nu = 30$ (left), 20 (middle) and 10 (right), respectively. The physical regions of the momentum transfer taken to be $Q^2_-(W_{\rm cut}) \le Q^2 \le Q^2_+(W_{\rm cut})$.

multiplying the SM hadronic current (45) by k^ν and q^ν, see Appendix B, we have

$$F_T = \frac{-iF}{\sqrt{q^2}}. \tag{47}$$

One can find the details of the decay rate calculations in Appendix A. We find that $\Gamma_{\rm SM} = 5.5 \times 10^{-13}$ GeV. The total decay rate of τ is $\Gamma_{\rm tot} = 2.27 \times 10^{-12}$ GeV, so that $\mathrm{BR}(\tau^- \to \nu_\tau + \pi^- + \pi^0)$ is 24.23% in our calculations which is close to the experimental result $(25.52 \pm 0.09)\%$ [30]. Using the CVC hypothesis, it is predicted that $\mathrm{BR}(\tau^- \to \pi^-\pi^0\nu_\tau) = (24.75 \pm 0.38)\%$ [29].

From the constraint $\tau^- \to \pi^-\pi^0\nu_\tau$, we find that $0.07 < |T_L| < 0.2$ within the 2σ level. If we take the tensor coupling to be complex, the contour plot in Fig. 3 shows the allowed region of the real and imaginary components of the coupling for the measured $\tau \to \pi^-\pi^0\nu_\tau$ within the 2σ level. The SM expectation for the branching ratio is not allowed within the experimental range at the 2σ level but it is allowed at higher standard deviation level.

In the explicit leptoquark models, $S_L(m_{\rm LQ}) = \pm 4T_L(m_{\rm LQ})$, one can obtain the constraint on S_L and T_L from $\tau^- \to \nu_\tau\pi^-$ and $\tau^- \to \pi^-\pi^0\nu_\tau$ at the same time within the limits of $0.07 < |T_L| < 0.2$ and $0.62 < |S_L| < 1.73$ within the 2σ level. The allowed regions of the real and imaginary components are shown in the contour plot in Fig. 4.

The $\pi\pi$ state is produced dominantly though an intermediate vector resonance and is in a P wave. Therefore, the scalar terms with the couplings S_L and S_R do not contribute to the decay process $\tau^- \to \nu_\tau\pi^-$ as the scalar hadronic current vanishes because of parity.

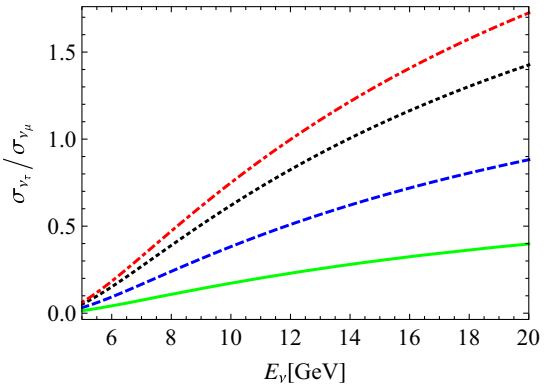

FIG. 15 (color online). $V \pm A$ model: The ratio between the total cross section of $\nu_\tau + N \to \tau + X$ to $\nu_\mu + N \to \mu + X$ in the $V \pm A$ model. The green lines correspond to the standard model predictions $V_L = V_R = 0$. The blue, black, and red lines correspond to $(V_L, V_R) = (0.4596, 0.4504)$, (0.8189,0.8082), (0.9836,0.9731).

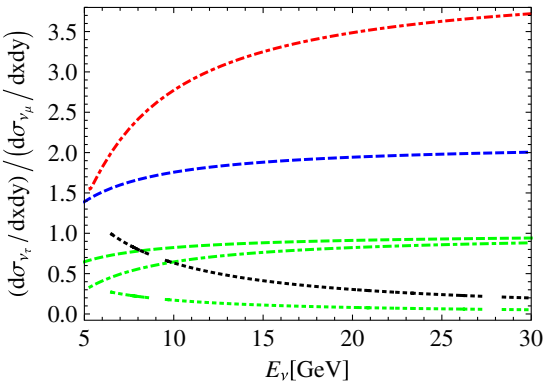

FIG. 16 (color online). $V \pm A$ model: The ratio between the differential cross section $(d\sigma/dxdy)$ of $\nu_\tau + N \to \tau + X$ to $\nu_\mu + N \to \mu + X$ in the $V \pm A$ model. The green lines correspond to the standard model predictions $V_L = V_R = 0$. The blue, black, and red lines correspond to $(V_L, V_R) = (0.4596, 0.4504), (0.8189, 0.8082), (0.9836, 0.9731)$. The blue and green dashed lines correspond to $(x, y) = (0.95, A + B)$. The red and green dot dashed lines correspond to $(x, y) = (0.475, (A + B)/2)$. The black and green dotted lines correspond $(x, y) = (\frac{m_\tau^2}{2M(E_\nu - m_\tau)}, A - B)$.

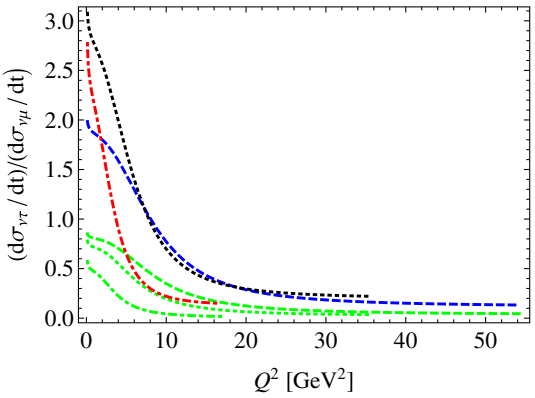

FIG. 17 (color online). $V \pm A$ model: The ratio between the differential cross section $(d\sigma/dt)$ of $\nu_\tau + N \to \tau + X$ to $\nu_\mu + N \to \mu + X$ in the $V \pm A$ model. The green lines correspond to the standard model predictions $V_L = V_R = 0$. The blue, black, and red lines correspond to $(V_L, V_R) = (0.4596, 0.4504)$, (0.8189,0.8082), (0.9836,0.9731) at $E_\nu = 30$, 20, 10, respectively. The physical regions of the momentum transfer taken to be $Q^2_-(W_{\rm cut}) \le Q^2 \le Q^2_+(W_{\rm cut})$

In the $V \pm A$ case, the couplings can be constrained by both $\tau^- \to \nu_\tau + \pi^-$ and $\tau \to \pi^- + \pi^0 + \nu_\tau$ decays. Considering the first process the branching ratio is given as

$$\mathrm{Br}^{\pi}_{V\pm A} = \mathrm{Br}^{\pi}_{\rm SM}(1 + r^{\pi}_{V\pm A})^2, \tag{48}$$

where the $V \pm A$ contribution is

$$r^{\pi}_{V\pm A} = V_L - V_R. \tag{49}$$

From the second process, the branching ratio is given as

$$\mathrm{Br}^{\pi\pi}_{V\pm A} = \mathrm{Br}^{\pi\pi}_{\rm SM}(1 + r^{\pi\pi}_{V\pm A})^2, \tag{50}$$

where the $V \pm A$ contribution is

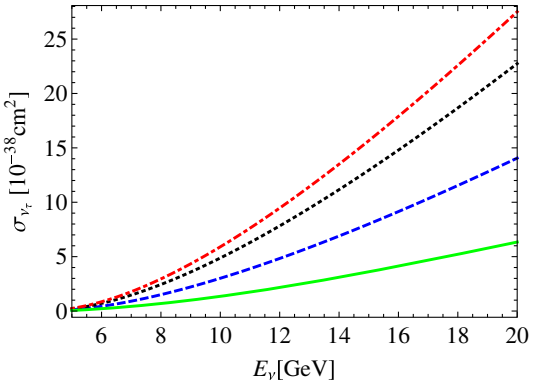

FIG. 18 (color online). $V \pm A$ model: The total cross section of $\nu_\tau + N \to \tau + X$ in the $V \pm A$ model. The green lines correspond to the standard model predictions $V_L = V_R = 0$. The blue, black, and red lines correspond to $(V_L, V_R) = (0.4596, 0.4504)$, (0.8189,0.8082), (0.9836,0.9731).

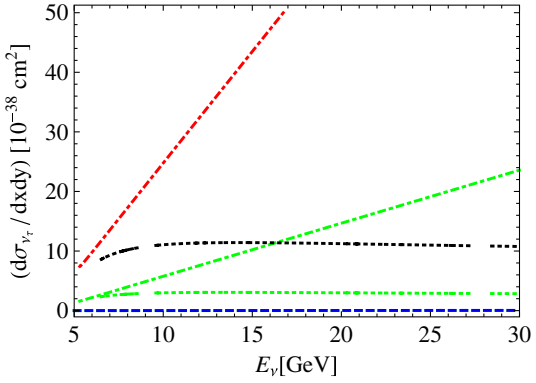

FIG. 19 (color online). $V \pm A$ model: The differential cross section $(d\sigma/dxdy)$ of $\nu_\tau + N \to \tau + X$ in the $V \pm A$ model. The green lines correspond to the standard model predictions $V_L = V_R = 0$. The blue, black, and red lines correspond to $(V_L, V_R) = (0.4596, 0.4504)$, (0.8189,0.8082), (0.9836,0.9731). The blue and green dashed lines correspond to $(x, y) = (0.95, A + B)$. The red and green dot dashed lines correspond to $(x, y) = (0.475, (A + B)/2)$. The black and green dotted lines correspond to $(x, y) = (\frac{m_\tau^2}{2M(E_\nu - m_\tau)}, A - B)$.

$$r^{\pi\pi}_{V\pm A} = V_L + V_R. \tag{51}$$

If we take the couplings to be real, the contour plot in Fig. 5 shows the allowed region. The allowed regions for the real and imaginary parts, if the couplings are taken to be complex, are shown in the contour plot in Fig. 6. This figure makes a circular contour plot, but the figure shows a part of it.

Note, even though we consider complex couplings in the constraint equations in this section, we take the couplings to be real for the scattering calculations.

IV. NUMERICAL ANALYSIS

In this section the sensitivity of the neutrino cross-section experiments to the scalar and tensor interactions, explicit leptoquark model, and $V \pm A$ interactions is discussed. We study the ratio of the total cross section, $d\sigma/dxdy$, and $d\sigma/dt$ for the tau-neutrino to the muon-neutrino scattering. We also show the results of the total cross section, $d\sigma/dxdy$, and $d\sigma/dt$ for the process $\nu_\tau + N \to \tau + X$.

A. Scalar and tensor interactions

The ratio of the total cross section is shown in Fig. 7 while the ratio of the differential cross sections $d\sigma/dxdy$ and $d\sigma/dt$ are given in Figs. 8–9. The impact of the new physics is clearly detectable in the ratio of the total cross section and the differential cross sections. The new physics effect is also observable in the total cross section, $d\sigma/dxdy$, and $d\sigma/dt$ for the process $\nu_\tau + N \to \tau + X$, as shown in Figs. 10–12.

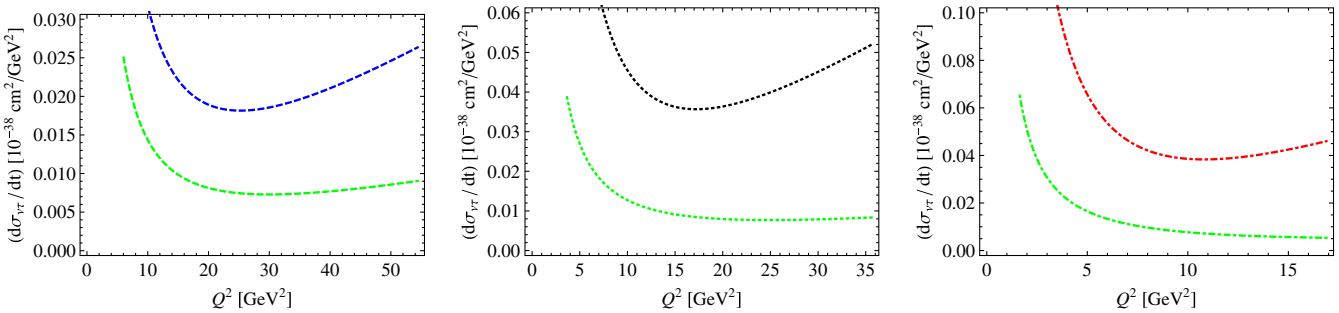

FIG. 20 (color online). $V \pm A$ model: The differential cross section $(d\sigma/dt)$ of $\nu_\tau + N \to \tau + X$ in the $V \pm A$ model. The green lines correspond to the standard model predictions $V_L = V_R = 0$. The blue, black, and red lines correspond to $(V_L, V_R) = (0.4596, 0.4504)$, (0.8189,0.8082), (0.9836,0.9731) at $E_\nu = 30$(left), 20(middle), 10(right), respectively. The physical regions of the momentum transfer taken to be $Q^2_-(W_{\rm cut}) \le Q^2 \le Q^2_+(W_{\rm cut})$.

B. Explicit leptoquark model

Here we take $m_{\rm LQ} = 1$ TeV. In Figs. 13–14, we show the differential cross section $d\sigma/dt$ and its ratio for the particular models $S_L(m_{\rm LQ}) = \pm 4T_L(m_{\rm LQ})$. The impact of the new physics is clearly detectable.

C. $V \pm A$ interactions

The ratio of the total cross section, $d\sigma/dxdy$, $d\sigma/dt$ are shown in Figs. 15–17, respectively. The figures show that it is possible to distinguish the presence of the $V \pm A$ contribution in the neutrino cross section measurements. The new physics effect is the same in the total cross section, $d\sigma/dxdy$, and $d\sigma/dt$ for the process $\nu_\tau + N \to \tau + X$, as shown in Figs. 18–20.

V. CONCLUSION

In this paper we discussed tests of lepton nonuniversal interactions through ν_τ scattering. We adopted an effective Lagrangian description of new physics and considered explicit leptoquark models for our calculations. The parameters of the new physics were constrained by single pion and two pion τ decays, $\tau^-(k_1) \to \nu_\tau(k_2) + \pi^-(q)$ and $\tau(p) \to \pi^-(p_1) + \pi^0(p_2) + \nu_\tau(p_3)$, which are well measured. We then discussed the ratio of the total and differential cross sections for the two deep inelastic scattering processes $\nu_\tau + N \to \tau + X$ and $\nu_\mu + N \to \mu + X$ as a probe of the new physics in the neutrino cross-section experiments. In the ratio of cross sections, the uncertainty of the parton distribution functions is expected to cancel out leading to precise results. In the effective Lagrangian framework we looked at models with scalar and tensor interactions. As an explicit realization of such models we considered leptoquark models where scalar and tensor couplings arise with relations between the couplings. We also considered vector-axial vector new physics operators in our analysis. Our results showed significant new physics effects, both in the total cross sections as well as in the differential distributions for $\nu_\tau + N \to \tau + X$, are allowed with the present constraints. These new physics effects could be observed at future proposed ν_τ scattering experiments.

ACKNOWLEDGMENTS

This work was financially supported in part by the National Science Foundation under Grant No. NSF PHY-1414345 (A.D and H.L).

APPENDIX A: TWO-PIONS DECAY

Here, we give details of the calculations of the process $\tau(p) \to \nu_\tau(p_3) + \pi^-(p_1) + \pi^0(p_2)$. In the rest frame of π^- and π^0,

$$p = (E, \ \vec{P}), \qquad p_1 = (E_1, \ \vec{P}_1),$$
$$p_2 = (E_2, \ -\vec{P}_1), \qquad p_3 = (E_3, \ \vec{P}), \tag{A1}$$

$$k = p_1 - p_2 = (E_1 - E_2, \ 2\vec{P}_1),$$
$$q = p_1 + p_2 = (E_1 + E_2, \ 0), \tag{A2}$$

and we define two variables,

$$m_{12}^2 = (p_1 + p_2)^2 = q^2,$$
$$m_{23}^2 = (p_2 + p_3)^2. \tag{A3}$$

Then,

$$d\Gamma = \frac{1}{(2\pi)^3}\frac{1}{32m_\tau^3} X dm_{12}^2 dm_{23}^2, \tag{A4}$$

with

$$X = \frac{1}{2}\sum_{\rm spin}|M_{\rm SM} + M_T|^2 = \frac{1}{2}\sum_{\rm spin}|M_{\rm SM}|^2 + \frac{1}{2}\sum_{\rm spin}|M_T|^2, \tag{A5}$$

where $M_{\rm SM}$ and M_T are given in Eqs. (43), (44), and the cross terms are zero.

By averaging the spin, we can get

$$X_{\rm SM} = 4G_F^2 V_{ud}^2 F^2(Q^2)[2(k\cdot p)(k\cdot p_3) - k^2(p\cdot p_3)], \tag{A6}$$

and,

$$X_T = 16G_F^2V_{ud}^2T_L^2\frac{F^2(Q^2)}{q^2}[(k\cdot q)^2(-p\cdot p_3)+2(k\cdot q)((k\cdot p_3)(p\cdot q)+(k\cdot p)(p_3\cdot q)) - 2q^2(k\cdot p)(k\cdot p_3)+k^2(q^2(p\cdot p_3)-2(p\cdot q)(p_3\cdot q))]. \quad (A7)$$

All these $X's$ can be expressed in terms of m_{12}^2 and m_{23}^2 because

$$E_1 = \frac{m_{12}^2-m_2^2+m_1^2}{2m_{12}}, \quad (A8)$$

$$E_2 = \frac{m_{12}^2-m_1^2+m_2^2}{2m_{12}}, \quad (A9)$$

$$E_3 = \frac{M^2-m_{12}^2-m_3^2}{2m_{12}}, \quad (A10)$$

$$E = \frac{M^2+m_{12}^2-m_3^2}{2m_{12}}, \quad (A11)$$

$$2\vec{p}_1\cdot\vec{p} = m_{23}^2-m_2^2-m_3^2-2E_2E_3, \quad (A12)$$

$$|\vec{p}| = \sqrt{E^2-M^2}, \quad (A13)$$

$$|\vec{p}_1| = \sqrt{E_1^2-m_1^2}, \quad (A14)$$

with $M = m_\tau = 1.77$ GeV, $m_1 = m_{\pi^-} = 0.140$ GeV, $m_2 = m_{\pi^0} = 0.135$ GeV, $m_3 = m_{\nu_\tau} = 0$.

Let us work on the SM case first and set

$$A_1 = k\cdot p = E(E_1-E_2)-2\vec{p}_1\cdot\vec{p} = E(E_1-E_2)+2E_2E_3+m_2^2+m_3^2-m_{23}^2, \quad (A15)$$

$$A_2 = k\cdot p_3 = E_3(E_1-E_2)-2\vec{p}_1\cdot\vec{p} = E_3(E_1-E_2)+2E_2E_3+m_2^2+m_3^2-m_{23}^2, \quad (A16)$$

$$A_3 = k^2 = (E_1-E_2)^2-4\vec{p}_1{}^2 = (E_1-E_2)^2-4(E_1^2-m_1^2), \quad (A17)$$

$$A_4 = p\cdot p_3 = E_1E_3-\vec{p}^2 = E_1E_3-E^2+M^2. \quad (A18)$$

Then,

$$X_{\rm SM} = 4G_F^2V_{ud}^2F^2(Q^2)[2A_1A_2-A_3A_4], \quad (A19)$$

Now, let us integrate $X_{\rm SM}$ by m_{23}^2 within the limits

$$(m_{23}^2)_{\max} = (E_2+E_3)^2-\left(\sqrt{E_2^2-m_2^2}-\sqrt{E_3^2-m_3^2}\right)^2, \quad (A20)$$

$$(m_{23}^2)_{\min} = (E_2+E_3)^2-\left(\sqrt{E_2^2-m_2^2}+\sqrt{E_3^2-m_3^2}\right)^2, \quad (A21)$$

where $m_1 = m_2 = m_\pi$, $m_{12}^2 = Q^2$ and $M = m_\tau$. One can get

$$\Gamma_{\rm SM} = \frac{4G_F^2m_\tau^5}{96(2\pi)^3}\frac{\cos\theta_c}{2}\int_{Q_{\min}^2}^{Q_{\max}^2}\frac{dQ^2}{m_\tau^2}F^2(Q^2) \times\left(1-\frac{Q^2}{m_\tau^2}\right)^2\left(1+2\frac{Q^2}{m_\tau^2}\right)\left(1-\frac{4m_\pi^2}{Q^2}\right)^{3/2}. \quad (A22)$$

Now, we can integrate over m_{12}^2 within the limits

$$Q_{\max}^2 = (m_{12}^2)_{\max} = (M-m_1)^2, \quad Q_{\min}^2 = (m_{12}^2)_{\min} = (m_1+m_2)^2. \quad (A23)$$

Now let us work on the tensor leptoquark case, we set

$$B_1 = k\cdot q = E_1^2-E_2^2, \quad (A24)$$

$$B_2 = p\cdot p_3 = EE_3-\vec{p}^2, \quad (A25)$$

$$B_3 = k\cdot p_3 = E_3(E_1-E_2)-2\vec{p}\cdot\vec{p}_1, \quad (A26)$$

$$B_4 = p\cdot q = E(E_1+E^2), \quad (A27)$$

$$B_5 = k\cdot p_3 = E(E_1-E_2)-2\vec{p}\cdot\vec{p}_1, \quad (A28)$$

$$B_6 = P_3\cdot q = E_3(E_1+E_2), \quad (A29)$$

$$B_7 = q^2 = (E_1+E_2)^2, \quad (A30)$$

$$B_8 = k^2 = (E_1-E_2)^2-4\vec{p}_1{}^2. \quad (A31)$$

Then,

$$X_T = 8G_F^2V_{ud}^2T_L^2F_T^2(q^2)[-B_1^2B_3+2B_1(B_3B_4+B_1B_6) - 2B_7B_1B_5+B_8(B_7B_2-2B_4B_6)]. \quad (A32)$$

Similarly, we can get $\Gamma_T = 3.43\times10^{-12}T_L^2$ GeV.

APPENDIX B: HADRONIC CURRENTS

In the decay process $\tau^- \to \nu_\tau + \pi^-$, the SM hadronic current is given in Eq. (34). By multiplying the current by $q^\mu = p_d^\mu + p_u^\mu$, one can find the NP scalar current is given by

$$\langle 0|\bar{d}(A_S - B_S\gamma^5)u|\pi(q)\rangle = \frac{i\sqrt{2}f_\pi m_\pi^2}{m_u + m_d}B_S. \tag{B1}$$

If one multiplies the SM current by $k^\mu = p_d^\mu - p_u^\mu$, the scalar current will be

$$\langle 0|\bar{d}(A_S - B_S\gamma^5)u|\pi(q)\rangle = i\sqrt{2}f_\pi(m_u + m_d)B_S. \tag{B2}$$

Now, by multiplying the two equations above and taking the square root, we end up with scalar current that is independent of the quark masses

$$\langle 0|\bar{d}(A_S - B_S\gamma^5)u|\pi(q)\rangle = i\sqrt{2}f_\pi m_\pi B_S. \tag{B3}$$

In the process $\tau^-(p) \to \pi^-(p_1) + \pi^0(p_2) + \nu_\tau(p_3)$, the NP tensor current is given in Eq. (46). Here $p_1^\mu = p_d^\mu + p_q^\mu$ and $p_2^\mu = p_u^\mu - p_q^\mu$, where p_u and p_d are the momenta of the up and down quarks that come from the tau decay, and $(p_q, -p_q)$ are the momenta of the quark-antiquark pair from the vacuum that pair up with the up and down quarks to form π^0 and π^-. By multiplying the current by $q^\mu = p_1^\mu + p_2^\mu = p_d^\mu - p_u^\mu$ and using the equation of motion, in the isospin symmetry limit, one gets the form factor

$$F_T = -i\frac{(m_u + m_d)}{q^2}F. \tag{B4}$$

If one multiply the tensor current by $k^\mu = p_1^\mu - p_2^\mu = p_d^\mu - p_u^\mu + 2p_q^\mu$, the form factor will be given by

$$F_T = \frac{-iF}{(m_d + m_u) - (1 - 2\frac{p_q\cdot k}{k^2})\left(\frac{m_{\pi^-}^2 - m_{\pi^0}^2}{m_d - m_u}\right)}. \tag{B5}$$

Now if the $\pi\pi$ is dominantly coming from a vector resonance then we can expect that the distribution of the momenta of the quarks inside the resonance will be peaked around $p_u = p_d$. In this limit the second term in the denominator above vanishes as $(1 - 2\frac{p_q\cdot k}{k^2}) = 0$. Hence, by taking the second term in the denominator small, we get

$$F_T = -i\frac{1}{(m_u + m_d)}F. \tag{B6}$$

Now, by multiplying the two equations above and taking the square root, then the form factor will be independent of the quark masses

$$F_T = \frac{-iF}{\sqrt{q^2}}. \tag{B7}$$

[1] J. P. Lees *et al.* (*BABAR* Collaboration), Evidence for an Excess of $\bar{B} \to D^{(*)}\tau^-\bar{\nu}_\tau$ Decays, Phys. Rev. Lett. **109**, 101802 (2012).

[2] J. P. Lees *et al.* (*BABAR* Collaboration), Measurement of an excess of $\bar{B} \to D^{(*)}\tau^-\bar{\nu}_\tau$ decays and implications for charged Higgs bosons, Phys. Rev. D **88**, 072012 (2013).

[3] S. Fajfer, J. F. Kamenik, and I. Nisandzic, On the $\bar{B} \to D^{(*)}\tau^-\bar{\nu}_\tau$ sensitivity to new physics, Phys. Rev. D **85**, 094025 (2012); Y. Sakaki and H. Tanaka, Constraints of the charged scalar effects using the forward-backward asymmetry on $B \to D^{(*)}\tau\bar{\nu_\tau}$, Phys. Rev. D **87**, 054002 (2013).

[4] See for instance, A. Datta, M. Duraisamy, and D. Ghosh, Diagnosing new physics in $b \to c\tau\nu_\tau$ decays in the light of the recent *BABAR* result, Phys. Rev. D **86**, 034027 (2012); M. Duraisamy and A. Datta, The full $B \to D^*\tau^-\bar{\nu_\tau}$ angular distribution and *CP* violating triple products, J. High Energy Phys. 09 (2013) 059; M. Duraisamy, P. Sharma, and A. Datta, The azimuthal $B \to D^*\tau^-\bar{\nu_\tau}$ angular distribution with tensor operators, Phys. Rev. D **90**, 074013 (2014); S. Shivashankara, W. Wu, and A. Datta, $\Lambda_b \to \Lambda_c\tau\bar{\nu}_\tau$ decay in the standard model and with new physics, Phys. Rev. D **91**, 115003 (2015).

[5] B. Bhattacharya, A. Datta, D. London, and S. Shivashankara, Simultaneous explanation of the R_K and $R(D^{(*)})$ puzzles, Phys. Lett. B **742**, 370 (2015).

[6] R. Aaij *et al.* (LHCb Collaboration), Test of lepton universality using $B^+ \to K^+\ell^+\ell^-$ decays, Phys. Rev. Lett. **113**, 151601 (2014).

[7] G. Hiller and F. Kruger, More model independent analysis of $b \to s$ processes, Phys. Rev. D **69**, 074020 (2004); C. Bobeth, G. Hiller, and G. Piranishvili, Angular distributions of $_{\bar{B}} \to K_{\bar{l}}$ /decays, J. High Energy Phys. 12 (2007) 040; C. Bouchard, G. Peter Lepage, C. Monahan, H. Na, and J. Shigemitsu (HPQCD Collaboration), Standard Model Predictions for $B \to K\ell^+\ell^-$ with Form Factors from Lattice QCD, Phys. Rev. Lett. **111**, 162002 (2013); **112**, 149902(E) (2014).

[8] See for example A. K. Alok, A. Dighe, D. Ghosh, D. London, J. Matias, M. Nagashima, and A. Szynkman, New-physics contributions to the forward-backward asymmetry in $B \to K^*\mu^+\mu^-$, J. High Energy Phys. 02 (2010) 053; A. K. Alok, A. Datta, A. Dighe, M. Duraisamy, D. Ghosh,

and D. London, New physics in $b \to s\mu^+\mu^-$: CP-conserving observables, J. High Energy Phys. 11 (2011) 121; New physics in $b \to s\mu^+\mu^-$: CP-violating observables, J. High Energy Phys. 11 (2011) 122.

[9] R. Aaij *et al.* (LHCb Collaboration), Measurement of Form-Factor Independent Observables in the Decay $B^0 \to K^{*0}\mu^+\mu^-$, Phys. Rev. Lett. **111**, 191801 (2013).

[10] See for example: A. Datta, M. Duraisamy, and D. Ghosh, Explaining the $B \to K^*\mu^+\mu^-$ anomaly with scalar interactions, Phys. Rev. D **89**, 071501 (2014).

[11] K. Kodama *et al.* (DONuT Collaboration), Final tau-neutrino results from the DONuT experiment, Phys. Rev. D **78**, 052002 (2008).

[12] A. Rashed, P. Sharma, and A. Datta, Tau neutrino as a probe of nonstandard interaction, Nucl. Phys. **B877**, 662 (2013); A. Rashed, M. Duraisamy, and A. Datta, Nonstandard interactions of tau neutrino via charged Higgs and W' contribution, Phys. Rev. D **87**, 013002 (2013).

[13] E. Graverini, N. Serra, and B. Storaci, Search for new physics in SHiP and at future colliders, JINST 10 (**2015**) 7007; D. Gorbunov, A. Makarov, and I. Timiryasov, Decaying light particles in the SHiP experiment: Signal rate estimates for hidden photons, Phys. Rev. D **91**, 035027 (2015).

[14] T. Bhattacharya, V. Cirigliano, S. D. Cohen, A. Filipuzzi, M. Gonzalez-Alonso, M. L. Graesser, R. Gupta, and H.-W. Lin, Probing novel scalar and tensor interactions from (ultra)cold neutrons to the LHC, Phys. Rev. D **85**, 054512 (2012); C.-H. Chen and C.-Q. Geng, Lepton angular asymmetries in semileptonic charmful B decays, Phys. Rev. D **71**, 077501 (2005).

[15] A. Datta, P. J. O'Donnell, Z. H. Lin, X. Zhang, and T. Huang, Effects of Kaluza-Klein excited W on single top quark production at Tevatron, Phys. Lett. B **483**, 203 (2000).

[16] S. Kretzer and M. H. Reno, Tau neutrino deep inelastic charged current interactions, Phys. Rev. D **66**, 113007 (2002).

[17] C. H. Albright and C. Jarlskog, Neutrino production of M^+ and E^+ heavy leptons (I), Nucl. Phys. **B84**, 467 (1975).

[18] K. Hagiwara, K. Mawatari, and H. Yokoya, Tau polarization in tau neutrino nucleon scattering, Nucl. Phys. **B668**, 364 (2003); **701**, 405(E) (2004).

[19] W. Buchmuller, R. Ruckl, and D. Wyler, Leptoquarks in lepton-quark collisions, Phys. Lett. B **191**, 442 (1987); **448**, 320(E) (1999).

[20] F. S. Queiroz, K. Sinha, and A. Strumia, Leptoquarks, dark matter, and anomalous LHC events, Phys. Rev. D **91**, 035006 (2015).

[21] W. Buchmuller, R. Ruckl, and D. Wyler, Leptoquarks in lepton-quark collisions, Phys. Lett. B **191**, 442 (1987).

[22] I. Dorsner, S. Fajfer, N. Kosnik, and I. Nisandzic, Minimally flavored colored scalar in $\bar{B} \to D^{(*)}\tau\bar{\nu}$ and the mass matrices constraints, J. High Energy Phys. 11 (2013) 084.

[23] K. G. Chetyrkin, Quark mass anomalous dimension to $O(\alpha_s^4)$, Phys. Lett. B **404**, 161 (1997).

[24] J. A. Gracey, Three loop MS-bar tensor current anomalous dimension in QCD, Phys. Lett. B **488**, 175 (2000).

[25] K. Nakamura *et al.* (Particle Data Group), Review of particle physics, J. Phys. G **37**, 075021 (2010) and 2011 partial update for the 2012 ed.

[26] M. Davier, A. Hocker, and Z. Zhang, The physics of hadronic tau decays, Rev. Mod. Phys. **78**, 1043 (2006).

[27] B. C. Barish, Caltech Pasadena Report No. CALT-68-1580, 1989.

[28] J. H. Kuhn and A. Santamaria, τ decays to pions, Z. Phys. C **48**, 445 (1990).

[29] A. Bernicha, G. Lopez Castro, and J. Pestieau, S-matrix approach to two pion production in e + e- annihilation and τ decay, Phys. Rev. D **53**, 4089 (1996).

[30] K. A. Olive *et al.* (Particle Data Group), Review of particle physics, Chin. Phys. C **38**, 090001 (2014).